Potential Biomarkers of thyroid neoplasia: the impact of proteomics analysis in the diagnosis.

Summary

Fine-needle aspiration cytology (FNA) is the most important tool to correctly address a thyroid lesion. Thyroid cancers account for about 5% of all lesions. A correct diagnosis may be difficult using FNA. Thyroid biomarkers help to better characterized thyroid lesions. Among the new techniques, proteomics , since 2002, has been increasingly used. In this thesis we describe the results obtained by the proteomic analysis of thyroid FNA to detect potential biomarkers for thyroid neoplasia and its impact in clinical management of thyroid malignancies.

INTRODUCTION

The most important diagnostic approach to distinguish between benign and malignant thyroid nodules is represented by fine-needle aspiration cytology (FNA)[1,2]. Malignant thyroid tumors account for about 5% of all thyroid lesions[3,4]. A correct diagnosis of FNA samples may sometimes be difficult using the traditional tools[5-6]. Recently, the discovery of thyroid biomarkers has led to the identification of various proteins which help to better characterized thyroid lesions[6-8]. Among the new techniques, since 2002, proteomics has been used to differentiate thyroid malignancies from benign lesions[9-14]. The aim of this thesis is to describe the results obtained by the proteomic analysis of thyroid FNA to detect potential biomarkers for thyroid neoplasia and its impact in clinical management of thyroid malignancies.

PATIENT AND METHODS

Chemicals

Iodoacetamide (IAA), CHAPS, urea, thiourea, glycerol, SDS, TEMED, ammonium persulfate, glycine, 30% acrylamide-N,N,N-bisacrylamide, trifluoroacetic acid (TFA), HEPES and copper sulphate were acquired from Sigma-Aldrich (St. Louis, MO, USA). Sodium chloride (NaCl), acetonitrile (ACN) from J.T. Baker. Sodium acetate, Trizma base, SDS, DTT and trichloroacetic acid (TCA) from AppliChem. IPGs pH 3–10 NL, pharmalyte

3–10 NL and dry strip cover fluid were purchased from GE Health Care, Europe (Uppsala, Sweden). Coomassie Brilliant Blue G 250 was from Merck (Darmstadt, Germany). All other reagents were supplied by standard commercial sources and were of the highest grade available.

Patients

The study was conducted between October 2005 and April 2010. A full clinical evaluation and routine laboratory tests were performed and all patients. Inclusion criteria were represented by normal preoperative values of free F-T3, F-T4 and thyroid stimulating hormone (TSH). Detectable serum anti-thyroid peroxidase (Ab-TPO) and anti-thyroglobulin antibodies (Ab-Tg) were considered exclusion criteria to dismiss patients from the study. Therapy with L-thyroxine at the time of the surgery was also considered as an exclusion criterion. An informed consensus was obtained from all patients for diagnostic or clinical purposes. The study was approved by the local Ethics Committee. The normal and malignant nature of FNA samples was assessed by histological analysis[6]. Formalin-fixed and paraffin-embedded samples of thyroid tissues were stained by hematoxylin and eosin (E&E). Definitive diagnoses of benign lesion or thyroid carcinoma were performed in accordance with the guidelines of the World Health Organization (WHO) [3]. Seventy-seven patients were enrolled in the study. There were 15 males and

62 female patients. Mean age (years, ±SD) was 47.2 ±14.0 years (range 22-75). A surgical procedure of total thyroidectomy was achieved in all patients.

Sample collection and preparation

Immediately after surgical removal of the thyroid, a FNA with a 23G needle was performed by the surgeon on the suspected nodule. The same procedure was performed in the normal tissue (control sample) of the opposite lobe. After passing the needle through the tissue 3 or 4 times, 4 mL of saline solution were aspirated with the same syringe. This fluid collected was immediately centrifuged at 2300g for 20 min at 4 °C and processed. Proteins from resulting supernatants were precipitated using 10% (w/v) trichloroacetic acid (TCA) and 0.05% ditiothreitol (DTT). After incubation at 0 °C for 1 h, the insoluble material was pelleted at 14000g. The pellets were washed three times with pure acetone, air-dried and solubilized in 7 M urea, 2 M thiourea, 4% CHAPS, 60 mM DTT, 0.5% 3-10 ampholytes and 0.002% bromophenol blue (rehydration solution). The amount of protein was estimated by means of a RC DC protein assay from Bio-Rad. The protein amount was determined using Bio-Rad RC DC-protein assay. Bovine serum albumin (BSA) was used as a standard.

2-DE analysis

For analytical gels, 150 μg of proteins, for each sample, were filled up to 350 μl in 7M urea, 2M thiourea, 4% CHAPS, 60mM DTT, 0.5% 3-10 ampholytes and 0.002% bromophenol blue (rehydration solution). Isoelectrofocusing (IEF) was carried out by using 18 cm Immobiline Dry-Strips (GE Healthcare) with a non linear, pH 3-10, gradient. IEF was performed at 16°C on an Ettan IPGphor II apparatus (Amersham Biosciences), according to the following schedule: the samples were applied by in-gel rehydration for 10 h using low voltage (30 V), then the voltage was linearly increased from 200 to 5000 during the first 4 h, and then the proteins were focused for up to 70 000Vh at a maximum voltage of 8000 V. To prepare the IPG strips for the second dimension, the strips were first equilibrated 15 min at room temperature in a buffer containing 50 mM Tris-HCl, pH 8.8, 6 M Urea, 30% glycerol, 2% SDS, 0.002% bromophenol blue, 1% DTT, followed by a second equilibration for 10 min in the same buffer except that DTT was replaced by 2.5% IAA. Subsequently, the IPG strips were applied horizontally on top of 12.5% SDS-polyacrylamide gels (20x18x0.15 cm) and electrophoresis was performed using the PROTEAN-II Multi Cell system (Bio-Rad) with constant amperage (40mA/gel) at 10 °C until the dye front reached the bottom of the gel (about 5 h) applying a continuous buffer system.

Staining and image analysis

The analytical gels were stained with ammoniacal silver nitrate. The procedure of silver staining consisted of five sequential phases including protein fixation, sensitization, silver impregnation, image development and stopping. To ensure that the spot staining was within the values of the linearity range, the silver stain was performed in standard conditions of time and temperature. All solutions were kept at 4°C, except for silver solution, while room temperature was controlled at 18°C. All steps were performed on an orbital shaker. Briefly, at the end of the second dimension run, the gels were removed from the glass plates, washed in deionized water for 5 min, soaked in ethanol: acetic acid: water (40: 10: 50) for 1 hour and then soaked in ethanol: acetic acid: water (5: 5: 90) overnight. After protein fixation, the gels were washed in deionized water for 5 min at 4°C and soaked in a solution containing glutaraldehyde (1%) and sodium acetate (0.5 M) for 30 min. After washing 3 times in deionized water for 10 min at 4°C, the gels were soaked twice in a 2.7 naphtalene-disulfonic acid solution (0.05% w/v) for 30 min at 4 °C in order to obtain homogeneous dark brown staining of the proteins. Then the gels were rinsed 4 times in deionized water for 15 min at 4 °C. Staining was carried out in a freshly made ammoniacal (30%) silver nitrate (2.5%) solution for 30 minutes at 18 °C. After staining, the gels were washed 4 times in deionized water for 4 min at 4°C. The images were developed in a solution

containing citric acid (0.01% w/v) and formaldehyde (0.1% v/v) for 5 minutes. Development was stopped with a solution containing Tris (0.4M) and acetic acid (2% v/v). The stained gels were scanned using an Epson Expression 1680 Pro scanner and the images were analyzed using Image-Master 2D Platinum 6.01 (GE Health Care Europe, Uppsala). Spots were automatically detected, manually edited and then counted. After spot detection in gels, a match set and a synthetic image for each class was generated. A synthetic gel was obtained by averaging the positions, shapes, and optical densities of the matched spots in the set of gels class. This produces an intersection of all the gels, showing only the spots found in almost 75% of the images of each class.

Statistical analysis

The optical density of the proteins was expressed as a percentage of the volume, (mean ± SD) of the spots representing a certain protein that was determined in comparison with the total number of proteins present in the 2-DE gel. The significance of the differences (p value <0.05) was calculated using Mann-Whitney test.

Preparative gels

In order to identify proteins of interest, preparative gels are performed and stained with Coomassie Brilliant Blue G-colloidal. This detection method is

compatible with mass spectrometry but less sensitive than silver staining therefore, for preparative gels, we had to load 1500 μg of proteins. For first dimension, a preliminary step at 200 V for 12 h was introduced, while second dimension is the same as analytical gels. The preparative gels for mass spectrometric analysis were stained with Coomassie Brilliant Blue G-colloidal (0,12%Coomassie G-250, 10% ammonium sulfate, 2% phosphoric acid). Briefly, after protein fixation with acetic acid (7%) and methanol (40%) for 1 h, the gels were stained overnight with Coomassie Brilliant Blue G-colloidal diluted with methanol (4:1 v/v). The gels were then rinsed 60 seconds with a solution of acetic acid (10%) and methanol (25%) and finally washed twice for few seconds with a solution of methanol (25%). Both analytical and preparative gels showed the same protein pattern. Protein spots of interest were cut from gel and sent to Core Facility Proteomic (Université de Genève) for analysis by mass spectrometry and protein identification.

RESULTS

The first part of our experience was oriented in defining the proteomic profile of human thyroid FNA fluid. 2DE analysis was performed 17 patients (Ratio M:F 6:11, mean age (SD) 48.6(±14.0) years, range 22-75), 2DE analysis with silver staining allowed us to recognize about 220 protein's spot per sample (Fig. 1). Therefore a MALDI-TOF peptide mass fingerprint analysis was performed on 46 of these spots, identifying 30 different proteins. These latter

were classified by function (metabolic, antioxidative, pro-apoptotic, motility, other) or usual site (serum proteins). In some cases the same peptide was yielded by different spots, suggesting a post-transaltional modification. Table 1 summarize the proteins identified. Validation of findings was performed by means of Western Blot analysis for one protein of each class (Fig 2)[14].

Once obtained the proteome of human thyroid FNA, we performed a second trial comparing the proteomic analysis on all of the 77 patients (M:F 15:62, mean age 47.2±14.0 years, range 22-75) which had a preoperative diagnosis either suspicious or highly suggestive of a thyroid carcinoma (FNA Bethesda 4-6)[3,6]. Final diagnosis, as represented in (Table 2), was of classical variant of papillary carcinoma (cPTC) in 25 patients, follicular variant (PFV) in 15, tall cells variant (TCV) in 12, benign follicular lesion in 21. In the other 4 patients were found: 2 anaplastic thyroid carcinoma (ATC), 1 parathyroid carcinoma and 1 Riedel's thyroiditis. The latter was submitted to surgery for the suspicion of an anaplastic thyroid carcinoma. TCV patients showed extracapsular involvement in 50% of cases, thus confirming the higher aggressiveness of this variant. The proteomic profile on 2DE gel allowed finding qualitative and quantitative differences which characterized each variant of thyroid cancer from the control tissue. About 200-270 spots were identified (Fig.3a-3d). Peptide mass fingerprinting via MALDI-TOF mass spectrometry as well as Western Blot analysis were performed to quantify the

different expressions of each detected proteic spots respect to control tissue in cPTC and TCV. Detailed results are showed in Table 3. An up-regulation of 9 spots was found both ic cPTC and TCV. Between the two sub-type of cancer cPTC showed up-regulation of four more proteins: sorting nexin-5, moesin, galectin-3 and TTR precursor-spot 63, while in TCV 3 spots were exclusively up-regulated: TTR precursor-spot 56, beta actin, serum albumin. Moreover each subtype exclusively expressed some protein spots on 2DE gel: twelve spots in cPTC and three in TCV (circled spots in Fig.3a, 3b). A detailed comparison with cPTC, TCV and normal tissue helped to better clarify the up-regulation observed for each spot (Fig.4A-C).

The proteins profile of FNA of FVC well overlapped with those obtained from previous other variants of papillary cancer. Similar to PTC and TCV a significant up-regulation of specific functional proteins as glycolitic enzymes, serum and structural proteins was oserved when compared to control tissue. Specifically was found an increase of ferritin light chain (FLC)($p=0.029$), protein DJ-1 ($p=0.0475$) and cofilin-1 ($p=0.0021$) confirming the potential role of these proteins in thyroid cancer progression (Fig.3c).

The patient in whom a Riedel's thyroiditis (RT) was diagnosed by final histology was a 72-years old woman admitted for a clinical and ultrasound findings suspicion of ATC (Fig.5). The 2DE gel was compared to those of an ATC (Fig.6). Three proteins which were found to be up-regulated in thyroid

cancer (ferritin heavy chain (FHC), FLC, and haptoglobin) were evaluated. Protein expression in Riedel's patients and control tissue did not show significative differencies (p= 0.37, 0.73, 0.11 respectively for haptoglobin, FLC and FHC), while in ATC expression of haptoglobin, FLC and FHC respect RT was significantly increased (p=0.037, 0.035 and 0.047 respectively).

DISCUSSION

Proteomic analysis allowed us to define the human thyroid proteome, providing moreover an imaging patter specific for thyroid normal tissue[14]. Starting from this pattern we compared FNA samples of sub-type of thyroid carcinoma to define the eventual changing presented in protein expression[15]. An up-regulation of nine proteins specific protein in all papillary carcinomas and moreover four and three proteins exclusively expressed by cPTC and TCV respectively was found.

Analyzing the pattern of proteins hyper-expression our study confirmed the earlier findings by Brown and Torres Cabala regarding the upregulation for moesin, annexin A1 and gal-3 as well as for FLC, DJ-1 and TTR already described for cold nodule or thyroid cancer[9,11-13,15]. Particularly high levels of annexin A1 were reported by Petrella comparing well-differentiated and non-differentiated thyroid cancers, suggesting the role of this protein as a tumor suppressor gene, correlating with the degree of tumor differentiation[16]. The

role of annexin family seems to be confirmed also by the recent report of Jung in which the degree of downregulation of annexin A3 expression (sub-type of the group of annexins) correlates with tumor progression in papillary thyroid carcinoma[17].

Proteomics analysis allowed us to detect in all of the sub-types of cancer evaluated an up-regulation of structural protein respect to control. All the three variant (cPTC, TCV, FCV) presented significant increased expression of Cofilin ($p=0.018$, $p=0.012$, $p=0.0021$, respectively) respect to control[15]. Cofilin regulates actin polymerization and depolymerization during cell migration, thus directly affecting tumor invasion, thus its different expression within the sub-types might indicate a different degree of aggressiveness[15,18].

In cPTC exclusively S100A13 up-regulation was found. The S100 protein family is a Ca2+ binding protein superfamily, with 25 different peptides found in humans so far[19]. S100A13 is involved in non-classical pathway transmembrane transport of fibroblast growth factor-1 (FGF-1) and interleukin-1a, which are involved in angiogenesis, tumor growth, and cell proliferation and differentiation[19]. Specifically, S100A13 acts in the non-classical (non-vesicular) release of FGF-1 [19,20]. FGF-1, is a potent mitogen and angiogenic protein as a participant in the initiation, development and metastasis of tumors[19,20]. The importance of S100 family in tumor progression has been widely described by different reports in tumorigenesis and thyroid

cancer aggressiveness[11,21-24]. Brown determined by immunohistochemistry the hyper-expression of S100-A6 in thyroid malignancies[11], while Sofiadis recently reported its up-regulation in papillary thyroid cancer (especially in those with a history of previous irradiation) but not in follicular thyroid cancer[22]. Moreover Nipp found a correlation in between the expression of S100-A10 and S100-A6 and the lymph node metastasis in patients affected by papillary carcinoma. So far S100A13 overexpression may be considered, in the pattern of S100 family's actions, as a key factor for cell proliferation and tumor progression in cPTC.

A significant up-regulation of 6-fold to respect with controls was also found exclusively in cPTC regarding gal-3, confirming the role of this glycoprotein as a biomarker for thyroid carcinoma, as already stated by other authors[11,12,25,26].

The TTR precursor presented two spot (marked 56 and 63) but each spot was more expressed in only one of the two variants. The two spots showed a different molecular weight (respectively of 13 and of 34 KDa); the two different forms are respectively a monomeric TTR (spot 56) and a oligomeric TTR (spot 63). TTR-56 corresponded to a monomeric form typical of TCV, while TTR-63, is an oligomeric form due to strong non-covalent interaction between monomers, displayed in cPTC[15-17]. The expression of one of the two

forms might be related to the different oxidative status or protease activity in the specific cancer subtype[15].

Focusing on TCV three proteins were exclusively over-expressed FHC, peroxiredoxin-1 (PRX1) and 6-phosphogluconate dehydrogenase (6-GHPD). FHC showed an increase of 711-fold. It is well known that FHC plays a key role in protecting cells from oxidative stress[27]. Thus the level of over-expression of this protein may correlate with tumor progression and being a useful marker for TCV[15]. On the other hand PRX1 itself may concur to the effects of FHC, because of its role against oxidative stress, inducing an antiapoptotic effect, resulting in abnormal cell proliferation. 6GHPD is one of the regulatory factors in the redox pentose phosphate pathway. Hence its role may be linked to FHC and PRX1 to provide protection to neoplastic cells during tumor proliferation[15].

Regarding the patient with RT, a pre-operative work-up was inconclusive for a diagnosis and clinical exam suspected an anaplastic carcinoma. Proteomics of patient's samples demonstareted an expression of haptogloblin, FLC, and FHC comparable to the FNA of normal thyroid tissues, while in the AC 2DE an overexpression of > 100, > 500 and > 300 was found respectively[28].

CONCLUSIONS

Our study demonstrated that proteomics may have a preminent role in differentiation the profile of thyroid nodules. A specific proteome profile has been found for many sub-types of well differentiated (cPTC, TCV, FCV) and anaplastic thyroid carcinoma (ATC) allowing to recognize those forms harbouring a clinical higher aggressiveness compared to cPTC, but for which usually diagnosis is made only with pathological examination. Although not already included in the common clinical practice, the introduction of proteomic study on thyroid FNA might help the surgeon to tailor the proper care on the patient.

REFERENCES

1. Gharib H, Goellner JR. Fine-needle aspiration biopsy of the thyroid: an appraisal. Ann Inter Med 1993, 118: 282-289.

2. Diamantis A, Magiorkinis E, Koutselini H. Fine-needle aspiration (FNA) biopsy: historical aspects. Folia Histochem Cytobiol. 2009, 47: 191-197.

3. DeLellis RA, Llyoyd RV, Heitz PU, Eng C. 2004 World Health Organization Classification of Tumours: Pathology and Genetics of Tumours of Endocrine Organs; IARC Press: Lyon, France, 2004.

4. Lundgren CI, Zedenius J, Skoog L. Fine-needle aspiration biopsy of benign thyroid nodules: an evidence-based review. World J Surg 2008; 32: 1247-1252.

5. Zeiger MA, Dackiw AP. Follicular Thyroid lesions, elements that affect both diagnosis and prognosis. J Surg Oncol 2005; 89(3): 108-113.

6. Cibas ES, Ali SZ. The Bethesda System for Reporting Thyroid Cytopathology. Am J Clin Pathol 2009; 132: 658-665.

7. Prasad LM, Pellegatta SN, Huang Y, Nagaraja NN, De la Chapelle A, Kloos TR. Galectin-3, fibronectin-1, CITED-1, HBME1 and cytokeratin-19 immunohistochemistry is useful for the differential diagnosis of thyroid tumors. Mod Pathol 2005; 18(1): 48-57.

8. Santoro M, Melillo RM, Carlomagno F, Vecchio G, Fusco A. Minireview: RET: normal and abnormal functions. Endocrinology 2004; 145(12): 5448-5451.

9. Srisomsap C, Subhasitanont P, Otto A, Mueller EC, Punyarit P, Wittman-Liebold B, vasti J. Detection of cathepsin B upregolation in neoplastic thyroid tissue by proteomic analysis. Proteomics 2002, 2(6): 706-712.

10. Suriano R, Lin Y, Ashok BT, Schaefer SD, Schantz SP, Geliebter J, Tiwari RK. Pilot study using SELDI-TOF-MS based proteomic profile for the identification of diagnostic biomarkers of thyroid proliferative disease. J Proteome Res 2006; 5(4): 856-861.

11. Brown LM, Helme Sm, Hunsucker SW, Neta-Maier RT, Chiang SA, Heinz DE, Shroyer KR, Duncan MW, Haugen BR. Quantitative and qualitative differences in protein expression between papillary thyroid carcinoma and normal thyroid tissue. Mol Carcinog 2006; 45(8): 613-626.

12. Torres-Cabala C, Bibbo M, Panizo-Santos A, Barazi H, Krutzsch H, Roberts DD, Merino MJ. Proteomic identification of new biomarkers and application in thyroid cytology. Acta Cytol 2006; 50(5): 518-528.

13. Krause K, Karger S, Schierhorn A, Poncin S, Many MC, Fuhrer D. Proteomic profiling of cold thyroid nodules. Endocrinology 2007; 148(4): 1754-1763.

14. Giusti L, Iacconi P, Ciregia F, Giannaccini G, Basolo F, Donatini G, Miccoli P, Lucacchini A. Proteomic analysis of human thyroid fine needle aspiration fluid. J Endocrinol Invest 2007; 30: 865-869.

15. Giusti L, Iacconi P, Ciregia F, Giannaccini G, Donatini GL, Basolo F, Miccoli P, Pinchera A, Lucacchini A. Fine-needle aspiration of thyroid nodules: proteomic analysis to identify cancer biomarkers. J Proteome Res. 2008 Sep;7(9):4079-88. Epub 2008 Jul 30.

16. Petrella A, Festa M, Ercolino SF, Zerilli M, Stassi G, Solito E, Parente L. Annexin-1 downregulation in thyroid cancer correlates to the degree of tumor differentiation. Cancer Biol Ther. 2006 Jun;5(6):643-7. Epub 2006 Jun 11.

17. Jung EJ, Moon HG, Park ST, Cho BI, Lee SM, Jeong CY, Ju YT, Jeong SH, Lee YJ, Choi SK, Ha WS, Lee JS, Kang KR, Hong SC. Decreased annexin A3 expression correlates with tumor progression in papillary thyroid cancer. Proteomics Clin Appl. 2010 May;4(5):528-37. doi: 10.1002/prca.200900063. Epub 2010 Feb 26.

18. Wang W, Mouneimne G, Sidani M, Wyckoff J, Chen X, Makris A, Goswami S, Bresnick AR, Condeelis JS. The activity status of cofilin is directly related to invasion, intravasation, and metastasis of mammary tumors. J Cell Biol. 2006 May 8;173(3):395-404. Epub 2006 May 1.

19. Cao R, Yan B, Yang H, Zu X, Wen G, Zhong J. Effect of human S100A13 gene silencing on FGF-1 transportation in human endothelial cells. J Formos Med Assoc. 2010 Sep;109(9):632-40.

20. Jouanneau J, Moens G, Montesano R, et al. FGF-1 but not FGF-4 secreted by carcinoma cells promotes in vitro and in vivo angiogenesis and rapid tumor proliferation. Growth Factors 1995;12910:37–47.

21. Torres-Cabala C, Panizo-Santos A, KrutschHC, Barazi H, Namba M, Sakaguchi M, Roberts DD, Merino MJ. Differential expression of S100C in thyroid lesions. Int J Surg Pathol 2004; 12: 107-115

22. Sofiadis A, Dinets A, Orre LM, Branca RM, Juhlin CC, Foukakis T, Wallin G, Höög A, Hulchiy M, Zedenius J, Larsson C, Lethiö J. Proteomic Study of Thyroid Tumors Reveals Frequent Up-Regulaion of the Ca^{2+}-Binding Protein S100A6 in Papillary Thyroid Carcinoma. Thyroid 2010; 20(10): 1067-1076

23. Nipp M, Elsner M, Balluff B, Meding S, Sarioglu H, Ueffing M, Rauser S, Unger K, Höfler H, Walch A, Zitzelsberger H. S100-A10,

thioredoxin, and S100-A6 as biomarkers of papillary thyroid carcinoma with lymph node metastasis identified by MALDI Imaging. J Mol Med (Berl). 2011 Sep 22. [Epub ahead of print].

24. Danø K, Behrendt N, Høyer-Hansen G, Johnsen M, Lund LR, Ploug M, Rømer J. Plasminogen activation and cancer. Thromb Haemost. 2005 Apr;93(4):676-81. Review.

25. Bartolazzi A, Bellotti C, Sciacchitano S. Methodology and Technical Requirements of the Galectin-3 Test for the Preoperative Characterization of Thyroid Nodules. Appl Immunohistochem Mol Morphol. 2011 Jun 17. [Epub ahead of print]

26. Prasad ML, Pellegata NS, Huang Y, Nagaraja HN, de la Chapelle A, Kloos RT.Galectin-3, fibronectin-1, CITED-1, HBME1 and cytokeratin-19 immunohistochemistry is useful for the differential diagnosis of thyroid tumors. Mod Pathol. 2005 Jan;18(1):48-57.

27. Pham CG, Bubici C, Zazzeroni F, Papa S, Jones J, Alvarez K, Jayawardena S, De Smaele E, Cong R, Beaumont C, Torti FM, Torti SV, Franzoso G. Ferritin heavy chain upregulation by NF-kappaB inhibits TNFalpha-induced apoptosis by suppressing reactive oxygen species. Cell. 2004 Nov 12;119(4):529-42.

28. Iacconi P, Giusti L, Da Valle Y, Ciregia F, Giannaccini G, Torregrossa L, Proietti A, Donatini G, Mazzeo S, Basolo F, Lucacchini A. Can proteomic approach help us in diagnosis of Riedel's thyroiditis? A case report. In press.

FIGURES.

Fig.1. Results of 2DE (220 spots).

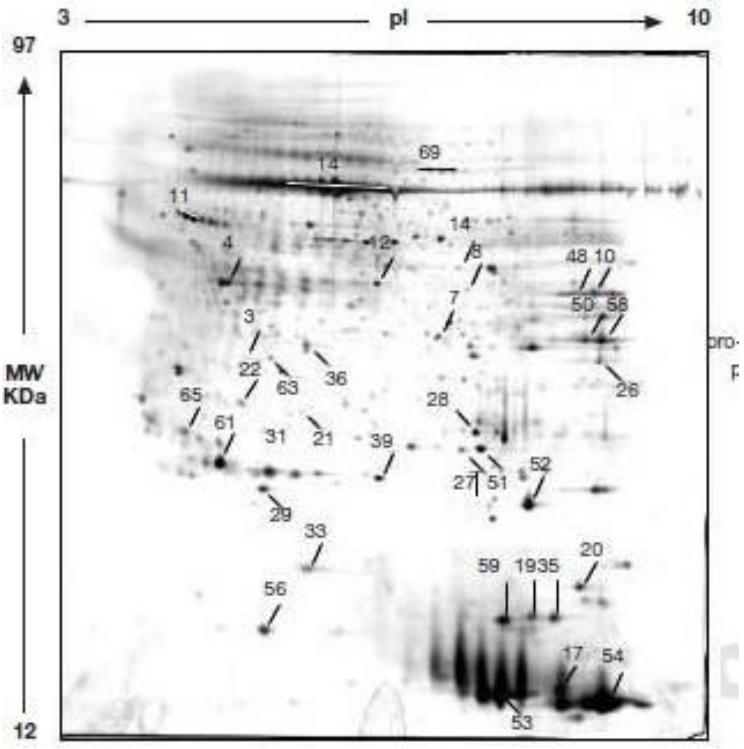

Fig.2. Validation of findings was performed by means of Western Blot analysis for one protein of each class.

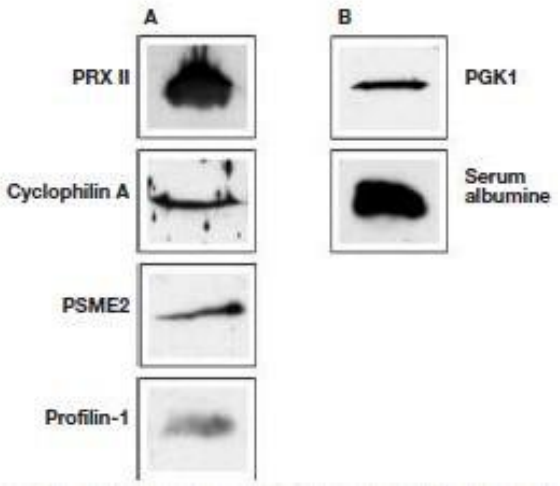

Fig. 3a-3d. 2DE pattern for cPTC, TCV, FVC and AP.

Fig. 3a. Papillary carcinoma classical variant (cPTC).

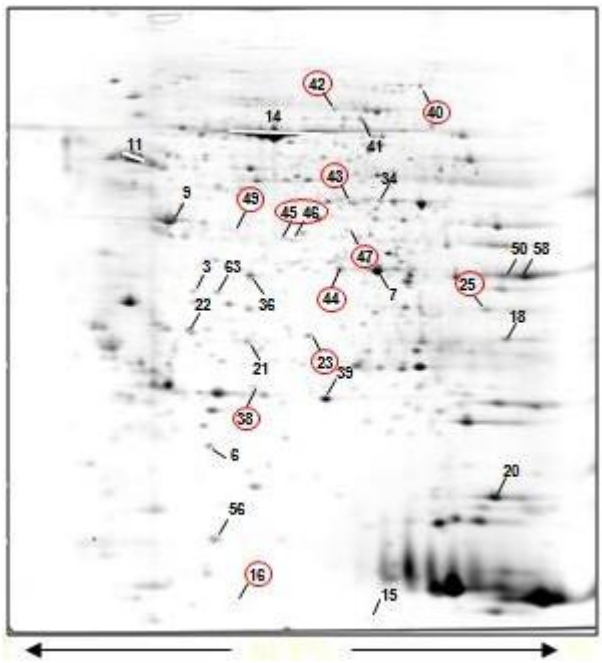

Fig. 3b. Papillary carcinoma tall cell variant (TCV).

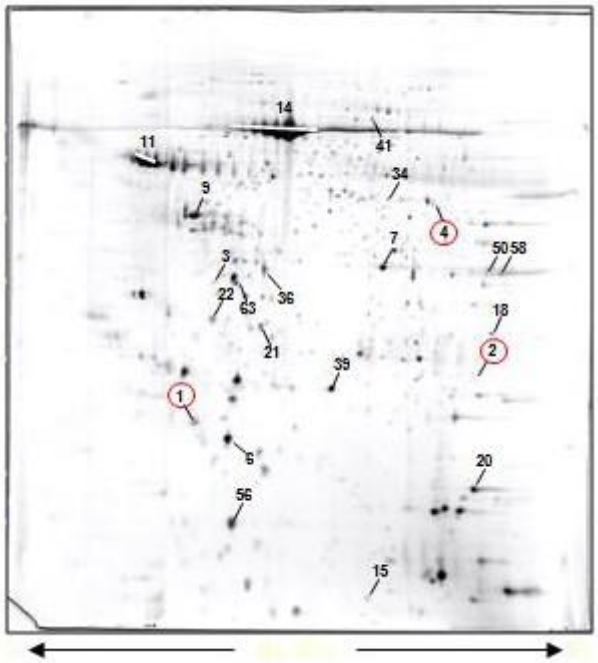

Fig. 3c. Papillary carcinoma. Follicular variant.

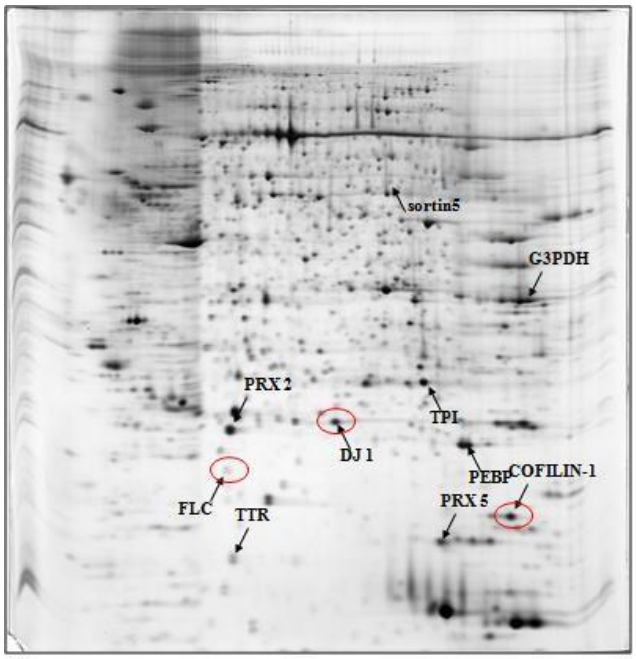

Fig. 3d. Anaplastic thyroid carcinoma (ATC).

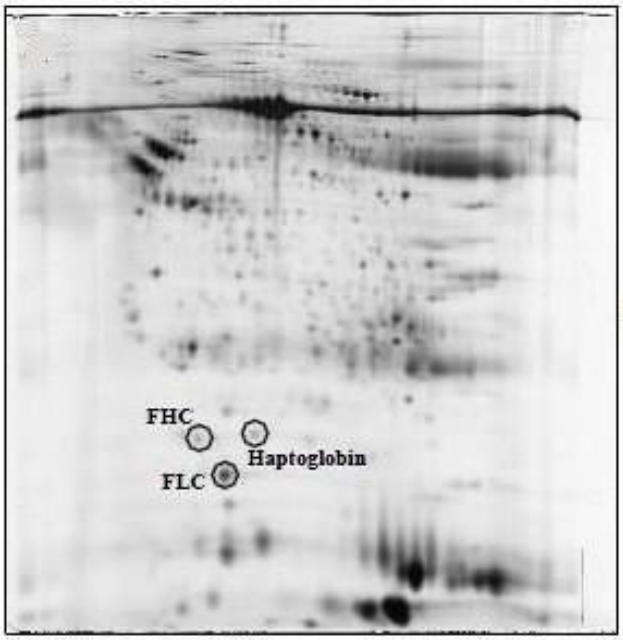

ig. 4. Detailed comparison between normal thyroid tissue (A), cPTC (B) and TCV (C), highlighting 2DE findings.

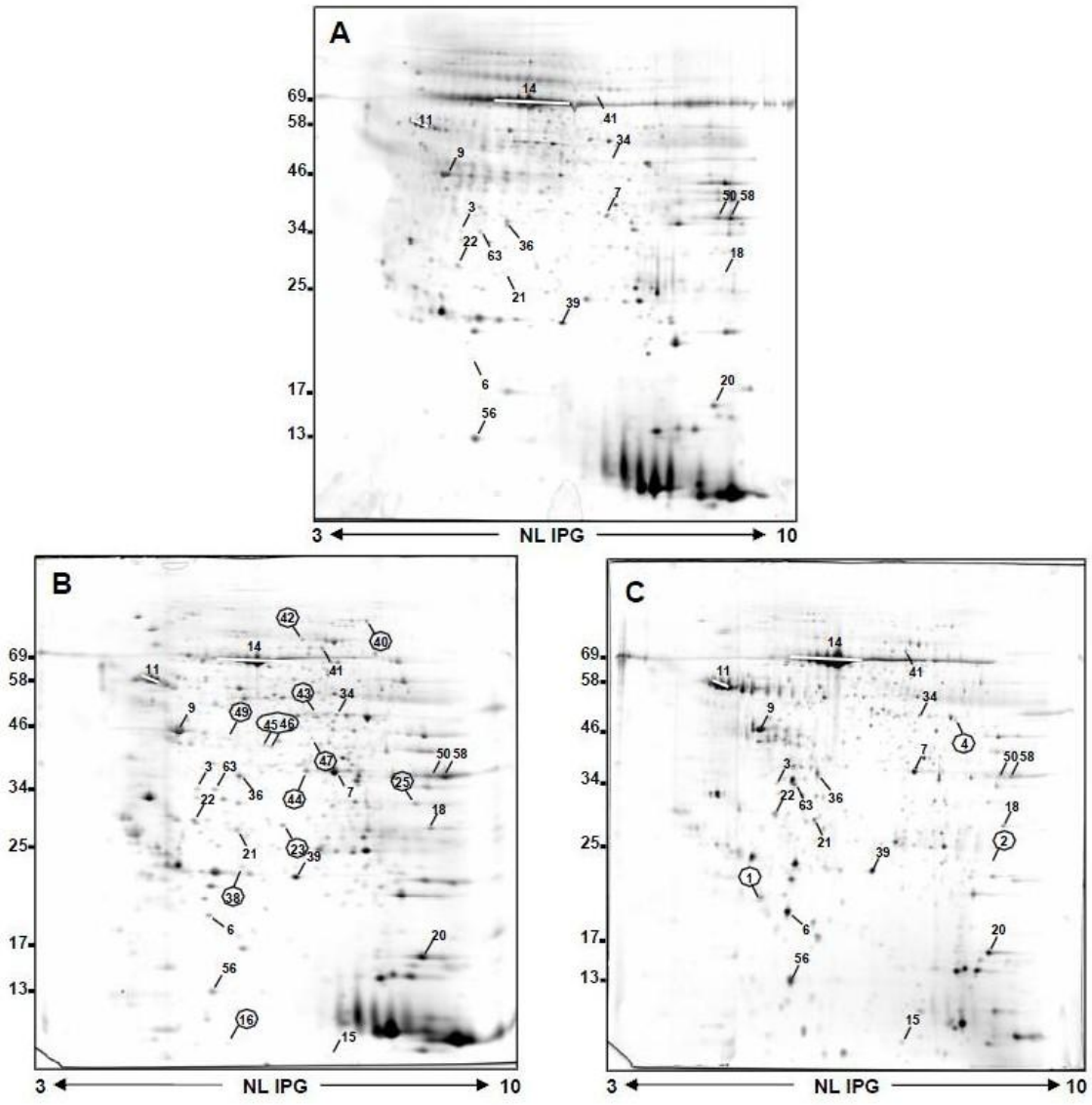

fig. 5. US findings in RT patients.

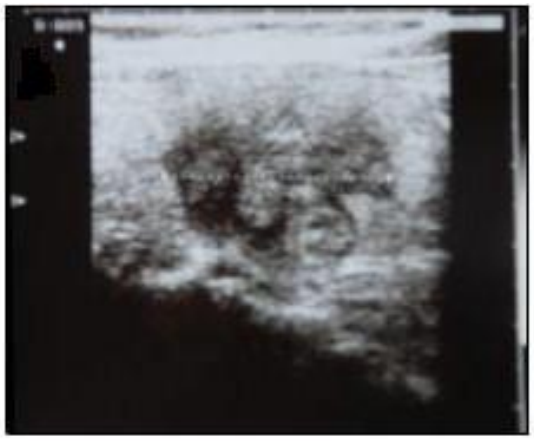

Fig. 6. 2DE comparing of RT(A), ATC(C) and normal thyroid tissue (B,D).

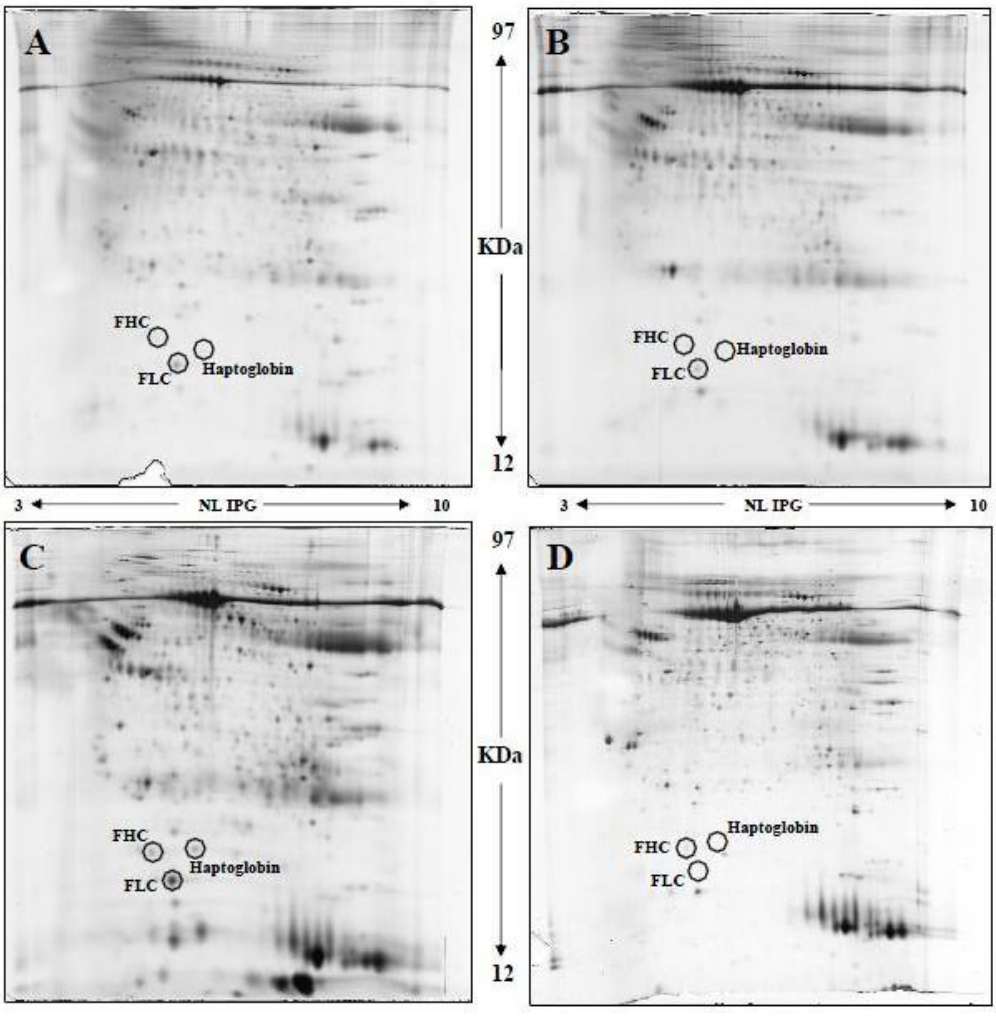

TABLES.

Table 1. Human proteomic profile in FNA fluid.

no. spot	protein name	Db entry	MW (kDa) th.	MW (kDa) obs.	pI th.	pI obs.	sequence coverage %	matched peptides	score
			Metabolism						
36	L-lactate dehydrogenase B chain	P07195	37	36	5.71	5.67	44	17	158
58	Glyceraldehyde-3-phosphate dehydrogenase	P04406	36	36	8.57	8.10	54	19	169
			Serum						
1	Ferritin heavy chain	P02794	21	20	5.30	5.27	59	10	111
6	Ferritin light chain	P02792	20	19	5.51	5.50	48	11	112
3	Apolipoprotein A-I precursor	P02647	31	34	5.56	5.40	30	8	57
11	Alpha-1-antitrypsin precursor	P01009	47	58	5.37	5.10	35	17	124
11	Alpha-1-antitrypsin precursor	P01009	47	57	5.37	5.00	36	18	157
11	Alpha-1-antitrypsin precursor	P01009	47	58	5.37	4.95	43	18	149
11	Alpha-1-antitrypsin precursor	P01009	47	58	5.37	4.88	45	22	192
14	Serum albumin precursor	P02768	71	69	5.92	5.61	58	39	317
14	Serum albumin precursor	P02768	71	68	5.92	5.65	72	22	314
14	Serum albumin precursor	P02768	71	67	5.92	5.70	69	22	323
14	Serum albumin precursor	P02768	71	66	5.92	5.75	66	37	358
14	Serum albumin precursor	P02768	71	66	5.92	5.80	69	46	365
14	Serum albumin precursor	P02768	71	66	5.92	5.89	74	36	296
56	Transthyretin precursor	P02766	16	13	5.52	5.52	69	8	104
63	Transthyretin precursor	P02766	16	34	5.52	5.55	73	9	116
			Stress						
2	Peroxiredoxin-1	Q06830	22	22	8.27	7.01	67	14	154
4	6-phosphogluconate dehydrogenase	P52209	54	49	6.80	6.65	29	16	126
38	Glutathione peroxidase 3 precursor	P22352	26	23	8.20	5.69	34	10	52
			Apoptosis						
7	Annexin A1	P04083	39	36	6.57	6.46	71	27	307
44	Annexin A1	P04083	39	39	6.57	6.17	61	24	243
21	Proteasome activator complex subunit 1	Q06323	29	28	5.78	5.66	49	16	108
22	Proteasome activator complex subunit 2	Q9UL46	28	29	5.44	5.38	61	18	149
39	DJ-1 Protein	Q99497	20	23	6.33	6.05	74	14	131
			Structural						
9	Beta Actin	Q96HG5	41	46	5.56	5.29	55	27	113
20	Cofilin-1	P23528	19	16	8.22	7.88	75	12	122
34	Sorting nexin-5	Q9Y5 × 3	47	54	6.31	6.43	50	18	134
41	Moesin	P26038	68	78	6.08	6.30	57	52	382
42	Villin 2 (Ezrin)	P15311	69	82	5.94	6.14	36	27	82
47	Septin 2	Q15019	42	47	6.15	6.23	61	24	190
			Others						
16	Protein S100 - A13	Q99584	12	11	5.93	5.60	48	6	67
18	Galectin-3	P17931	26	28	8.58	7.74	38	11	86
23	Chloride intracellular channel protein 3	O95833	27	27	5.99	6.03	77	19	209
25	Carbonyl reductase	P16152	31	32	8.55	7.51	30	8	45
40	Elongation factor 2	P13639	96	91	6.41	6.85	21	16	105
43	Elongation factor 1 gamma	P26641	50	53	6.25	6.23	26	14	102
46	Macrophage capping protein	P40121	39	45	5.88	5.89	41	13	87
49	Fibrinogen beta chain precursor	P02675	57	47	8.54	5.61	47	26	210
15	No identification	-	-	10	-	6.35	-	-	-
45	No identification	-	-	45	-	5.84	-	-	-

Table 2. Final diagnosis on pathological report.

Diagnosis	Number of Patients (n=77)
Papillary carcinoma classical variant (cPTC)	25
Papillary carcinoma follicular variant (PFV)	15
Papillary carcinoma tall cell variant (TCV)	12
Benign lesion	21
Anaplastic thyroid carcinoma (ATC)	4
Riedel's Thyroditis	1
Parathyroid carcinoma	1

Table 3. Differences between cPTC and TCV on proteins expression.

spot no.	protein name	mean ± SD			cPTC vs control		TCV vs control	
		control	cPTC	TCV	fold variation	*p*-value	fold variation	*p*-value
63	Transthyretin precursor	0.05 ± 0.03	0.21 ± 0.12	0.07 ± 0.14	3.9	0.0006	1.4	0.5273
56	Transthyretin precursor	0.54 ± 0.28	0.81 ± 0.54	1.15 ± 0.12	1.5	0.535	2.1	0.0121
39	DJ-1 Protein	0.26 ± 0.07	0.56 ± 0.17	0.48 ± 0.16	2.1	0.0006	1.8	0.0167
6	Ferritin light chain	0.005 ± 0.01	0.16 ± 0.13	3.58 ± 2.03	32	0.0006	711	0.0006
21	Proteasome activator complex subunit 1	0.09 ± 0.05	0.18 ± 0.14	0.31 ± 0.16	2	0.2593	3.5	0.0061
22	Proteasome activator complex subunit 2	0.09 ± 0.05	0.21 ± 0.10	0.37 ± 0.15	2.1	0.053	3.8	0.0061
11	Alpha-1-antitrypsin precursor	0.37 ± 0.29	1.16 ± 0.66	1.87 ± 0.46	3	0.0111	5	0.0061
58	GAPDH	0.18 ± 0.20	0.72 ± 0.49	0.56 ± 0.21	3.9	0.0221	3.1	0.0381
36	LDH-B	0.19 ± 0.04	0.49 ± 0.38	0.41 ± 0.15	2.5	0.0041	2.1	0.0167
20	Cofilin-1	0.36 ± 0.20	0.87 ± 0.36	1.14 ± 0.75	2.4	0.0175	3.2	0.0121
7	Annexin A1	0.06 ± 0.05	0.84 ± 0.47	0.37 ± 0.29	13	0.0006	5.7	0.0061
3	Apolipoprotein A1 precursor	0.02 ± 0.02	0.08 ± 0.03	0.13 ± 0.07	4.5	0.0023	7.6	0.0167
34	Sorting nexin-5	0.02 ± 0.02	0.07 ± 0.01	0.04 ± 0.04	5	0.0006	2.6	0.5273
41	Moesin	0.02 ± 0.04	0.11 ± 0.07	0.05 ± 0.05	5.4	0.0175	2.51	0.1636
18	Galectin-3	0.02 ± 0.03	0.11 ± 0.08	0.06 ± 0.08	6	0.0152	3	0.3524
9	Beta actin	0.31 ± 0.14	0.34 ± 0.36	0.80 ± 0.15	1.5	0.8048	2.6	0.0167
14	Serum albumin	1.57 ± 0.70	1.70 ± 1.04	3.20 ± 0.56	1.1	1.0000	2.04	0.0121